Results in Physics 24 (2021) 104108

Contents lists available at ScienceDirect

Results in Physics

journal homepage: www.elsevier.com/locate/rinp

Atomic population inversion and absorption dispersion-spectra driven by modified double-exponential quotient pulses in a three-level atom

N. Boutabba [a,*], S. Grira [b], H. Eleuch [c,d]

[a] Fatima College of Health Sciences, Institute of Applied Technology, Abu Dhabi, United Arab Emirates
[b] Department of Applied Sciences and Mathematics, Abu Dhabi University, Abu Dhabi, United Arab Emirates
[c] Department of Applied Physics and Astronomy, University of Sharjah, Sharjah, United Arab Emirates
[d] Institute for Quantum Science and Engineering, Texas A&M University, College Station, TX 77843, USA

ARTICLE INFO

Keywords:
Atomic population inversion
Absorption-dispersion Spectra
Modified QEXP pulse

ABSTRACT

In this study, we control a three-level atomic system using a typical strong control field with a modified quotient double exponential form (modified QEXP). The considered atomic configuration is a V-type three-level system in which QEXP is applied between the ground and excited states. Atomic population inversion can be achieved by selecting specific shaped pulses. In addition, we control the temporal atomic coherence of the system for a spectrum of waveforms and derive both absorption and dispersion spectra. Compared to a continuous wave control field, the proposed modified QEXP pulse achieves an electromagnetically induced transparency window in the absorption spectrum.

Introduction

The progress in the understanding of light-atom interactions has led to the development of techniques for the control of quantum systems, such as single atoms and quanta of light. This has attracted considerable interest because the atom-light interaction leads to atomic coherence that can be used to control the optical properties of an atomic medium. The achievement of a high laser population inversion, manipulation of atomic coherence, and control of the absorption-dispersion spectra in an atomic medium contributed to the development of various fields, including electromagnetically induced transparency (EIT) [1], lasing without inversion [2], atomic clocks [3], and coherent population trapping [4]. The studies have led to several applications including high resolution hyperfine spectroscopy [5], slowing light [6–9] and quantum memories[10,11]. For example, EIT has been studied experimentally and theoretically in three-level atoms to show that, in the presence of a strong control field in a certain frequency range, a highly absorptive medium may become transparent to the weak probe field [12].

A powerful approach to address the challenges related to the control of light is the use of pulse-shaping techniques. Several types of pulses can be produced in digital communications, such as rising cosine, sinc, root rising cosine, and Gaussian pulses. Such pulses can be chirped, which implies that the laser pulse can be stretched out temporally and spectrally, amplified, and then compressed again. Hence, since the advent of chirped pulse amplification techniques, notable progress has been achieved in the production of high-power femtosecond pulses and their applications. Recently, significant breakthroughs in lasers have been achieved [13]. An ultrashort chirped pulse has been directed through a lens generating a gradient force opposite to the direction of the beam and amplified by 11 orders of magnitude. This technique is referred to as optical tweezer trapping, applicable in biological and medical sciences [13].

Chirped laser pulses were applied to a three-level atom to produce an arbitrary coherent superposition of two ground states to store optical phase information [14]. In addition, several other studies have investigated atomic population transfer and optical coherence [15,16]. For high-power electromagnetic and ultra-wide-band pulse analysis, pulses of double exponential types, as well as their derivatives, are commonly used in digital communication. For example, the double exponential quotient (QEXP) [17] has been used in numerical simulations as a mathematical expression of high-altitude electromagnetic pulse (HEMP) environments [18] and pulse shapes of the gamma-ray source [19]. The shaping of the pulse in forms such as tan–hyperbolic, Gaussian, or complex cosine leads to distinct results in the three-level system (atomic population inversion, coherences, etc) [16].

In this study, we analyze a new pulse shape in a three-level atom with

* Corresponding author.
E-mail address: n_boutabba@yahoo.fr (N. Boutabba).

https://doi.org/10.1016/j.rinp.2021.104108
Received 9 January 2021; Received in revised form 18 March 2021; Accepted 18 March 2021
Available online 4 April 2021

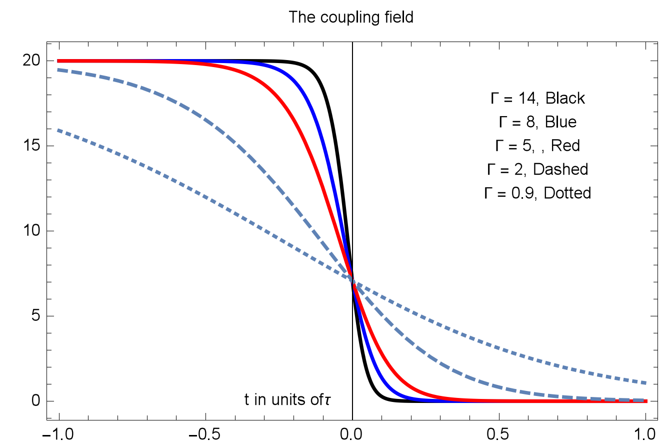

Fig. 1. Profiles of the modified quotient exponential wave forms.

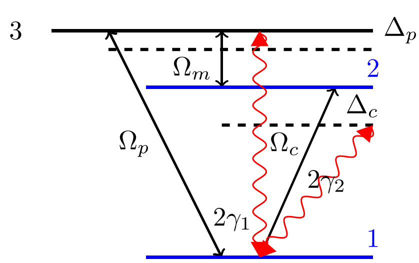

Fig. 2. Three-level atom.

a modified quotient exponential form, and report the atomic population inversion, temporal coherence, and dispersion-absorption spectra. In Section "Modified QEXP pulse", we describe the modified QEXP pump light followed by the atomic model in a three-level V-type configuration. In Section "Analysis", we analyze the atomic population inversion, coherence, and dispersion-absorption spectra.

Modified QEXP pulse

The (QEXP) waveforms have been used in numerical analyses as a mathematical representation of the pulse shapes of the (HEMP) and gamma-ray source [20,18]. In general, the analytical form of the QEXP pulses is:

$$f(t) = \frac{k}{e^{-\alpha t} + e^{\beta t}} \tag{1}$$

In Fig. 1, the modified QEXP pump laser is shown for different waveforms. The description and feasibility of this typical pulse is discussed in terms of α and β and their ratio in [17]. In addition, all possible realistic values for the realization of this shape are listed in Table II of [17].

In our study, we propose a typical pulse with a modified quotient of double exponential form expressed by:

$$\Omega(t) = \frac{\Omega_c e^{-3\Gamma t}}{(1 + e^{-2\Gamma t})^{\frac{3}{2}}} \tag{2}$$

where Γ is a variable, t is in the units of the pulse rise time, and Ω_c is the amplitude of the Rabi frequency used in our model. In the next sections, we investigate the pulse shape effects on the atomic population inversion, temporal coherence, and dispersion-absorption spectra of a typical three-level atomic medium.

We consider a V-type three-level configuration in which ground state $|1\rangle$ is coupled to the upper state $|2\rangle$ with a strong control field. The latter has a modified QEXP shape with a temporal Rabi frequency of $\Omega(t)$ and amplitude of Ω_c.

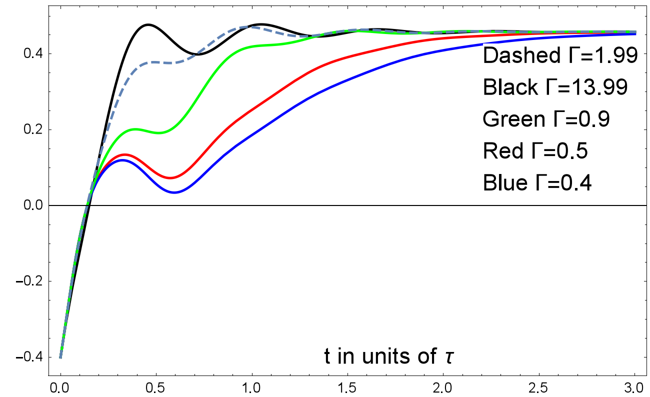

Fig. 3. Atomic population inversion dynamics for various modified QEXP wave forms.

We also consider a weak microwave field Ω_m that couples level pairs $|3\rangle$ to $|2\rangle$. Notably, this atomic scheme can be experimentally realized by an Rb^{87} atom with $5S_{1/2}$, F = 1, m = 1, $5P_{1/2}$, F = 1, m = 0 and $5S_{1/2}$, F = 2, m = 1 [21]. The radiative decay rates considered in this scheme are $\gamma_{1,2}$ from higher levels $|3\rangle$ to $|1\rangle$ and $|2\rangle$ to $|1\rangle$, as illustrated in Fig. 2. Under the rotating wave approximation, the Hamiltonian of the considered configuration is [16]:

$$H = \Delta_p|3\rangle\langle 3| + \Delta_c|2\rangle\langle 2| - (\Omega_c|2\rangle\langle 1| + \Omega_c^*|1\rangle\langle 2| + \Omega_p|3\rangle\langle 1| + \Omega_m|3\rangle\langle 2|) \tag{3}$$

where $\Delta_p = \omega_{31} - \omega_p$ and $\Delta_c = \omega_{21} - \omega_c$ denote the detunings of the probe and coupling fields, respectively. The temporal evolution of the system is expressed by the density matrix,

$$\begin{aligned}
\frac{d}{dt}\rho_{22} &= -2\gamma_2\rho_{22} + i\Omega_c(\rho_{12} - \rho_{21}) + i\Omega_m(\rho_{32} - \rho_{23}) \\
\frac{d}{dt}\rho_{33} &= -2\gamma_1\rho_{33} + i\Omega_p(\rho_{13} - \rho_{31}) + i\Omega_m(\rho_{23} - \rho_{32}) \\
\frac{d}{dt}\varrho_{21} &= -(\gamma_2 + i\Delta_c)\rho_{21} + i\Omega_c(\rho_{11} - \rho_{22}) - i\Omega_p\rho_{23} + i\Omega_m\rho_{31} \\
\frac{d}{dt}\varrho_{31} &= -(\gamma_1 + i\Delta_p)\rho_{31} + i\Omega_p(\rho_{11} - \rho_{33}) - i\Omega_c\rho_{32} + i\Omega_m\rho_{21} \\
\frac{d}{dt}\varrho_{32} &= -(\gamma_1 + \gamma_2 - i\Delta_c + i\Delta_p)\rho_{32} + i\Omega_p\rho_{12} - i\Omega_c\rho_{31} + i\Omega_m(\rho_{22} - \rho_{33})
\end{aligned} \tag{4}$$

where atomic populations are described by the diagonal elements, while coherences are described by the non-diagonal elements (because they describe the coherent oscillatory behavior of superpositions in the system). The atomic coherences in a medium are mathematically defined by the corresponding density matrix off-diagonal elements. In the density matrix formalism on the example of a two-level system of states $|i\rangle$ and $|j\rangle$, the element ρ_{ij} is related to the probability amplitude through the trace, which indicates coherence. ρ_{ij} is a complex number that includes the amplitude and phase in its real and imaginary parts, respectively [22].

Analysis

Atomic population inversion

To analyse the atomic population inversion, we consider that all Rabi frequencies are scaled by the decay rate γ_1. We set, $\gamma_1 = 1, \gamma_2 = 2\gamma_1, \Omega_p = 5$, and $\Omega_m = 2$. By numerically solving the above master equations, we analyze the temporal evolution of the atomic population inversion for different wave forms, denoted as $W = \rho_{33}(t) - \rho_{22}(t)$. We consider the case of Rb^{87}, where t is normalized in units of $\tau = \frac{1}{\gamma_1}$ (rubidium lifetime

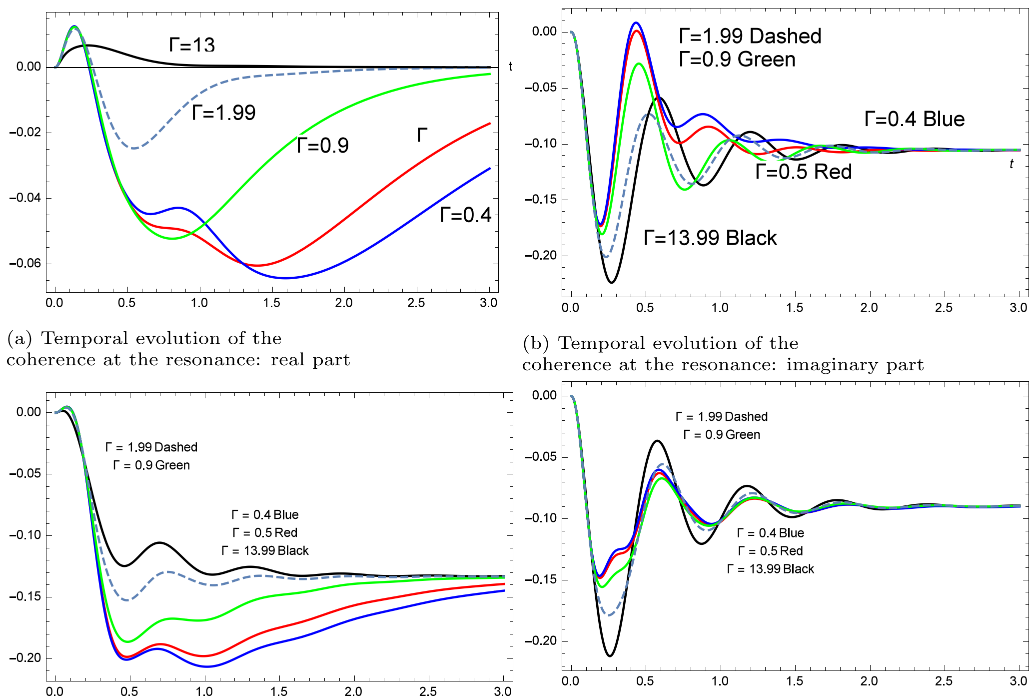

(a) Temporal evolution of the coherence at the resonance: real part

(b) Temporal evolution of the coherence at the resonance: imaginary part

(c) Temporal evolution of the coherence far from the resonance: real part

(d) Temporal evolution of the coherence far from the resonance: imaginary part far from the resonance

Fig. 4. Atomic coherence under modified QEXP pulses: ρ_{31} in terms of time t scaled to the pulse rise time.

and γ_1 is the decay rate) [23].

In Fig. 3, the atomic population inversion is presented for different waveforms of the modified QEXP pulse. All parameters were set for Rb^{87}. The atomic population inversion increases as the dropping edge of the input signal increases. Therefore, it is largely enhanced for a sharp waveform pulse that characterizes a waveform with a small fall time.

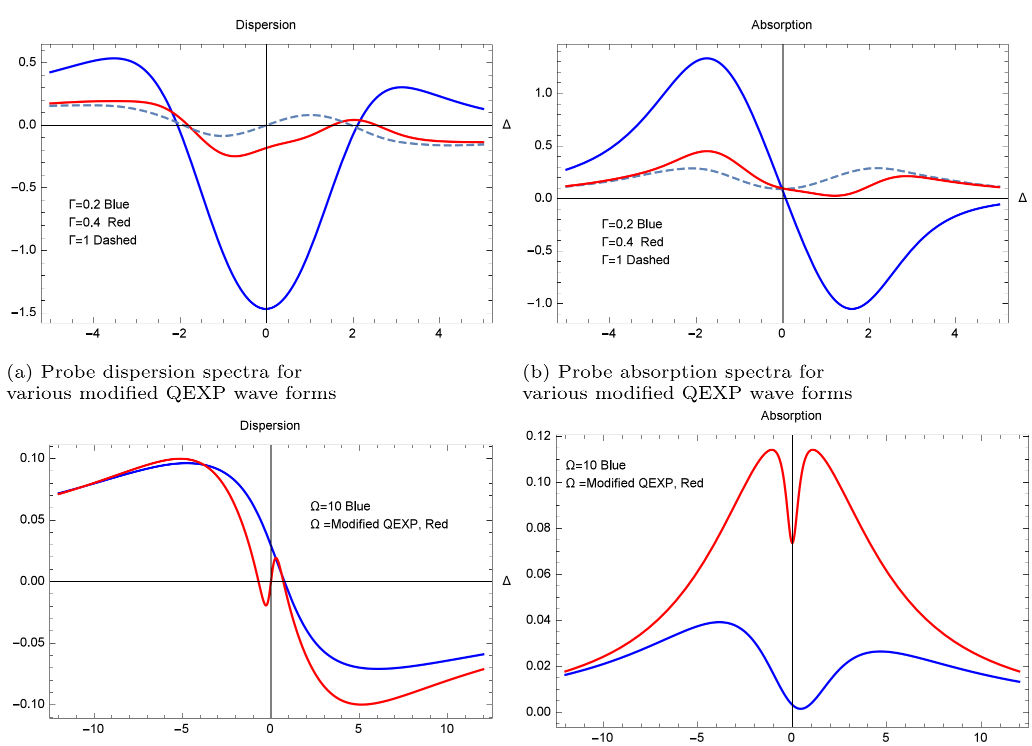

(a) Probe dispersion spectra for various modified QEXP wave forms

(b) Probe absorption spectra for various modified QEXP wave forms

(c) Dispersion spectra for a modified QEXP pulse (red curve), and constant control field (blue curve)

(d) Absorption spectra for a modified QEXP pulse (red curve), and constant control field (blue curve)

Fig. 5. Dispersion-absorption spectra.

Owing to the rapid drop pulse, a small resonant interaction time is required to produce the inversion.

Control of the coherence

In Fig. 4(a) and (b), we consider the case of resonance, where the frequency of the field coincides with the atomic transition frequencies. We present the real and imaginary parts of the coherence ρ_{31} in the atomic medium for various waveforms.

For each Γ-type waveform (Fig. 1), we generate a typical coherence. This implies that for each pulse shape we obtain a typical curve for coherence. Hence, the atomic coherence of the system is controlled by the pulse shape. In a practical scenario, the detection of a coherent interaction is complex as the electric field must satisfy numerous strict requirements. The two most significant requirements include the temporal and spatial structures of the field. Hence, to detect coherent effects, the pulse duration for a pulsed field must be shorter than the time constant of any decay mechanism. In the case where a chirped laser pumps the atoms from the ground state to the upper state, we control the coherences by varying the pulse shape, which is related to the pulse drop time.

Fig. 4(c) and (d), show the real and imaginary parts of the coherence far from the resonance, respectively. The detuning is scaled to the radiative decay constant [24]. In our case, $\Delta_p = 0.7\Delta_c$, and we observe that, out of resonance, the temporal dynamic process of the coherence is different from the resonance case. The real temporal coherence spectrum is less split away from the resonance, whereas the pulse form effect is less pronounced for the imaginary coherence (than for the resonant case).

Dispersion-absorption spectra

In this section, we describe the probe dispersion and absorption spectra. The dispersion is proportional to the real part of the off-diagonal density matrix element ρ_{31} while the absorption is proportional to its imaginary part. The spectra were derived in terms of the probe detuning. For different pulses, we obtained different spectra at the resonance, as illustrated in Fig. 5(a) and (b). Specific characteristics are observed in Fig. 5(c) and (d), showing the dispersion and absorption spectra, respectively, for a constant control field and for a modified QEXP control pulse. Under certain conditions ($\gamma_1 = 1.5$, $\gamma_1 = 0.5$, $\Gamma = 0.4$, $\Delta_p = 0.7\Delta_c, \Omega_p = \Omega_m = 2.$), the modified QEXP waveform leads to EIT window opening in a typical frequency range.

Conclusion

In this study, we investigated the effect of a typical modified QEXP laser pulse on the control of a three-level atomic medium. By solving the Bloch equations in the density matrix formalism and considering the rotating wave approximation, we analyzed the shape effect on the atomic population inversion, coherence, absorption and dispersion spectra at the resonance and out of resonance. The proposed pulse enables population inversion and directly relates the atomic coherence to the pulse time duration. By controlling the desirable waveforms, we can control the absorption and dispersion in the medium. An EIT window was achieved in the absorption spectrum by a control field with modified quotient of double exponential form.

Declaration of Competing Interest

The authors declare that they have no known competing financial interests or personal relationships that could have appeared to influence the work reported in this paper.

References

[1] Harris SE, Yin G, Kasapi A, Jain M, Luo Z. Electromagnetically induced transparency. In: Coherence and Quantum Optics VII. Springer; 1996. p. 295–304.

[2] Fry ES, Li X, Nikonov D, Padmabandu G, Scully MO, Smith AV, Tittel FK, Wang C, Wilkinson SR, Zhu S-Y. Atomic coherence effects within the sodium d 1 line: lasing without inversion via population trapping. Phys Rev Lett 1993;70(21):3235.

[3] Ludlow AD, Boyd MM, Ye J, Peik E, Schmidt PO. Optical atomic clocks. Rev Mod Phys 2015;87(2):637.

[4] Arimondo E. V coherent population trapping in laser spectroscopy. In: Progress in optics, Vol. 35, Elsevier, 1996, pp. 257–354.

[5] van Veldhoven J, Küpper J, Bethlem HL, Sartakov B, van Roij AJ, Meijer G. Decelerated molecular beams for high-resolution spectroscopy. Eur Phys J 2004;31 (2):337–49.

[6] Scheuer J, Paloczi GT, Poon JK, Yariv A. Coupled resonator optical waveguides: toward the slowing and storage of light. Opt Photon News 2005;16(2):36–40.

[7] Wang R, Ahmed I, Raza F, Li C, Zhang Y. Light slowing and all-optical time division multiplexing of hybrid four-wave mixing signal in nitrogen-vacancy center. Chin Phys B 2020.

[8] Boutabba N, Eleuch H. Slowing light control for a soliton-pair. Appl Math Inf Sci 2013;7(4):1505.

[9] Boutabba N, Eleuch H. Soliton propagation in three-level atomic system under detuned excitation. Opt Acoust Rev 2008;10(1):57.

[10] Simon C, Afzelius M, Appel J, de La Giroday AB, Dewhurst S, Gisin N, Hu C, Jelezko F, Kröll S, Müller J, et al. Quantum memories. Eur Phys J D 2010;58(1): 1–22.

[11] Yu Y, Ma F, Luo X-Y, Jing B, Sun P-F, Fang R-Z, Yang C-W, Liu H, Zheng M-Y, Xie X-P, et al. Entanglement of two quantum memories via fibres over dozens of kilometres. Nature 2020;578(7794):240–5.

[12] Li Y-Q, Xiao M. Electromagnetically induced transparency in a three-level λ)type system in rubidium atoms. Phys Rev A 1995;51(4):R2703.

[13] Asplund MC, Johnson JA, Patterson JE. The 2018 nobel prize in physics: optical tweezers and chirped pulse amplification. Anal Bioanal Chem 2019;411(20): 5001–5.

[14] Djotyan G, Bakos J, Sörlei Z. Three-level λatom in the field of frequency-chirped bichromatic laser pulses: Writing and storage of optical phase information. Phys Rev A 2001;64(1):013408.

[15] Rag HS, Gea-Banacloche J. Atomic population transfer for single-and n-photon wavepackets, JOSA B 38(1):s226–232.

[16] Boutabba N, Eleuch H. Quantum control of an optically dense atomic medium: Pulse shaping in a v-type three-level system. Res Phys 2020;19:103421.

[17] Wu G. Shape properties of pulses described by double exponential function and its modified forms. IEEE Trans Electromagn Compatib 2014;56(4):923–31.

[18] Baum CE. From the electromagnetic pulse to high-power electromagnetics. Proc IEEE 1992;80(6):789–817.

[19] Longmire CL, Hamilton RM, Hahn JM. A nominal set of high-altitude emp environments. Tech. rep. Santa Barbara, CA (USA): Mission Research Corp.; 1987.

[20] Xie Y. Modified description of early time high-altitude electromagnetic pulse waveform (e1). Sens Simul Notes 2013;562.

[21] Marte A, Volz T, Schuster J, Dürr S, Rempe G, Van Kempen E, Verhaar B. Feshbach resonances in rubidium 87: Precision measurement and analysis. Phys Rev Lett 2002;89(28):283202.

[22] Norsen T. Foundations of quantum mechanics. Springer; 2017.

[23] Steck DA. Rubidium 87 d line data (2001).

[24] Fleischhauer M, Imamoglu A, Marangos JP. Electromagnetically induced transparency: Optics in coherent media. Rev Mod Phys 2005;77(2):633.